

Contour-Variable Model of Constitutive Equations for Polymer Melts

Shuanhu Qi, Shuang Yang, and Dadong Yan*

Beijing National Laboratory for Molecular Sciences (BNLMS),

Institute of Chemistry, Chinese Academy of Sciences, Beijing 100190, China

(Dated: February 3, 2022)

Abstract

Based on a modified expression of the rate of the convective constraint release, we present a new contour-variable model of constitutive equations in which the non-uniform segmental stretch and the non-Gaussian chain statistical treatment of the single chain are considered to describe the polymer chain dynamics and the rheological behavior of an entangled system composed of linear polymer chains. The constitutive equations are solved numerically in the cases of steady shear and transient start-up of steady shear. The results indicate that the orientation and stretch, as well as the tube survival probability, have strong dependence on the chain contour variable, especially in the high-shear-rate region. However, the inclusion of the non-uniform features in the constitutive models has little modification comparing with the uniform models in determining the rheological properties both qualitatively and quantitatively.

Keywords: Constitutive equation, CCR, Contour variable, Polymer dynamics

* Corresponding author. Tel./Fax: +86-10-82617358; *E-mail:* yandd@iccas.ac.cn.

I. INTRODUCTION

Constitutive equations in polymer melts or concentrated solutions are mathematical relationships between the stresses and the external flow conditions. They represent the inherent properties of the polymer system, and should be derived from the knowledge of polymer chain structures, configurations, interactions and polymer dynamics. In practice, a constitutive model is needed to idealize these microscopic characteristics of polymer chains, due to the complex interactions of this many-chain system (Larson, 1988). As polymer melts own some characteristics of universality, that is to say, some physical properties of polymer melts are independent on the microscopic chemical structures, we can coarse grain a real polymer chain as a smooth thread connected by segments (Watanabe, 1999). This coarse-grained chain, just like the real chain, has an enormous number of configurations and can be usefully described statistically as Gaussian chain or non-Gaussian chain. In fact, the dynamics in our study is the segmental dynamics, which is based on a spatial scale of a chain segment and those chains are only distinguished by their lengths and abilities of extension. The interactions between chains are intricate. However, the attractive interactions between segments are tended to screen out by the excluded volume effect in polymer melts or concentrated solutions (de Gennes, 1979), leaving the topological constraints to play a dominant role in such a system at equilibrium. A basic understanding of chain dynamics is the key-point to develop constitutive equations for melts or concentrated solutions of flexible polymers. The proposition of the idea of ‘reptative’ motion by de Gennes (1971) is a milestone in the development of polymer dynamics of the concentrated system. In fact, in a flow the long linear polymer chains become oriented and stretched, which generates internal stress as the response to external disturbance. However, the orientation and stretch of chains will relax in the course of time due to the motion of non-crosslinked polymer chains. The major mechanisms of relaxation concerned are: reptation (Doi and Edwards, 1978a, b, c, 1979), convection of segments along primitive chains (Doi, 1980; Marrucci, 1986), fluctuations of the contour length (Doi and Edwards, 1986; Pearson and Helfand, 1984; Mead et al., 1998),

reptative constraint release (Marrucci, 1985; des Cloizeaux, 1988, 1990; Leygue et al., 2005, 2006a, b), and convective constraint release (CCR) (Marrucci, 1996; Ianniruberto and Marrucci, 1996; Milner et al., 2001; Graham et al., 2003). The first three kinds of relaxation are caused by the motion of the primitive chains, which can happen only at the ends; while the other two are induced by the motion of surrounding chains, which can occur not only at their ends but also in some other place along the primitive chains.

The optical-stress law guarantees a linear relationship between the stress and the orientational anisotropy of segments for a highly crosslinked rubber system (Treloar, 1975). The subsequent studies also show its validity for non-crosslinked polymer system (Janeschitz-Kriegl, 1975). The segments in the crosslinked rubber refer to chain portions between two permanently tethered crosslink points. The orientations of these segments are uniform. The segments in the non-crosslinked polymer system refer to entanglement segments. The orientations of these segments are non-uniform, as the segments can move freely. Under fast flow the polymer chains not only become oriented but also significantly stretched. The contribution from segmental stretch to stress is proportional to the square of stretch ratio for Gaussian chains (Doi and Edwards, 1986), while this relationship is much more complex for non-Gaussian chains. In the original Doi and Edwards (DE) model, due to the faster relaxation of segmental stretch, the chain is assumed to remain its equilibrium length all the time. The stress contribution comes only from segmental orientation. DE theory predicts a maximum in shear stress σ_{xy} with respect to the shear rate, and followed by a sharp decrease asymptotically as $\dot{\gamma}^{-0.5}$, which has not been observed by experiments. The neglect of segmental stretch results in a monotonic increase in the first normal stress difference in the start-up of a simple shear flow, however, an overshoot appears in experiment. In order to improve this deficiency of the original DE model, several ‘chain stretch’ models are proposed. In the uniform stretch model, it is assumed a uniform segmental stretch along the chain, such as Larson’s ‘partially convected strand’ model (1984) and also the one proposed by Pearson et al., (1989). The non-uniform segmental stretch model is proposed by Marrucci and Grizzuti (1988). The segmental stretch models are called as DEMG model (Mead and

Leal, 1995a, b). The extension of chain segments creates some segment (or saying pseudo *defect* (de Gennes, 1971)) sources along the chain, which is equivalent to reduce the diffusion coefficient. The inclusion of chain stretch also changes the feature in the start-up of shearing. A serious deficiency in all these models is that in the terminal region excessive shear thinning is inevitable due to the lacking of an extra relaxation mechanism to increase the rate of creating new segments, which is equal to the rate of annihilating old segments, or equivalently saying to avoid high orientation of the chain to the direction of flow. The Mead-Larson-Doi (MLD) model incorporating CCR to the DEMG model qualitatively improves the description of the phenomenon of excessive shear thinning and other rheological properties in steady state and transient shearing flow (Mead et al., 1998). Recently Patamaprom and Larson (2001) proposed a toy MLD model by making an extension of the MLD model in a simple way and adding reptative constraint release to MLD equations. In all these models, the rate of CCR is evaluated at the tube end, which is a uniform rate of CCR.

CCR represents the ability of the flow to convect or release entanglements, and is determined by segmental orientation and stretch. As the segmental orientation and stretch in the non-crosslinked polymer melts are non-uniform, the CCR is non-uniform. The rate of CCR is a function of both the contour variable and time. We assume that when the entanglement is convected away from the primitive chain segment to some other place, the previously formed environment has changed and this entanglement then becomes released. Based on this idea, we develop a new contour-variable model including non-uniform segmental stretch, non-uniform rate of CCR and non-Gaussian chain to describe the rheological behavior of linear chain entangled system in simple shearing and transient flows. However, we dropped the reptative constraint release term in the present work as we focus on the high-shear-rate region, where the segmental orientation and stretch are obvious. In the low-shear-rate region, the reptative constraint release occurs on a time scale of the reptation time of the whole chain and one event only relaxes a small part of the chain (Graham et al., 2003); while in the high-shear-rate region, the CCR dominates. Thus in both of these two cases it is valid to

drop the reptative constraint release term. While in some middle region, some quantitative deviations occur if we drop the reptative constraint release term. We also neglected the contribution from the fluctuations of the contour variable, as the problem is considered in the mean-field level.

This paper is organized as follows. In section II we develop a contour-variable dependent rate of CCR to describe the flow induced constraint release and construct the new equations which the segmental stretch and the tube survival probability satisfy, respectively. We promote our contour-variable model of constitutive equations in the end of this section. In section III we give the results and discussion, in which we focus on the simple steady shear flow and the start-up of steady shear flow. In section IV, we give the conclusions. The process and methods used for the calculation of constitutive equations are shown in the Appendix.

II. THE NEW CONTOUR-VARIABLE MODEL

A. Rate of CCR

CCR represents the entanglements relaxation mechanics caused by the convective motion of surrounding chains. It is not important when the concentrated system is at rest or undergoes a slow flow. However, when the velocity of the flow is comparable to the inverse of reptation time of the primitive chain, CCR will play a key role in determining the dynamics of the system. Taking into account the CCR mechanics, Ianniruberto and Marrucci (1996) proposed a contour location independent rate of CCR. In this model, the rate of CCR is only caused by the retraction of the primitive chain ends. So the rate of CCR is proportional to the velocity gradient of the movement of the primitive chain ends. However, not all convections or deformations will release constraint. In order to exclude the case of affine deformations, in which no constraint release occurs, Mead et al. gives the rate of CCR as the difference between the rate of convection of the entanglements and the rate of primitive chain retraction (Mead et al., 1998; Viovy et al., 1983). They only evaluate the rate of CCR

at the chain ends, since they think the topological constraint can be released only by the motion of chain ends (Ianniruberto and Marrucci, 1996; Marrucci et al., 2001). (We call it the end-relaxation mechanism in the follows.)

In the present work, we focus on the non-uniform behavior of CCR. Let us consider a primitive chain segment confined by a tube segment which was created at past time t' , as called the t' -segment. The deformation of this chain segment will be released when the entanglements forming the tube segments are convected away by the flow. It is an irreversible process. This t' -segment will never be created again. When this happens, some hidden entanglements become active (Ianniruberto and Marrucci, 2000), which instantaneously makes the released part (e.g. the t' -segment) become a part of a new tube. Thus we can say that the rate of creating a new segment is the same as that of annihilating an old segment. The contribution to the stress for a specified tube only comes from the part that remain unreleased. The released part of the original tube, which becomes a part of a new tube, will still have contributions to the stress. However, the stress should be calculated from the new tube. Define s_0 as the equilibrium contour variable, which runs from $-L_0/2$ to $L_0/2$, where L_0 is the equilibrium length of the primitive chain. When the chain is stretched, its primitive length L can be larger than L_0 . We then define a local stretch function $s(s_0, t)$ which takes the value from $-L/2$ to $L/2$, to describe the segmental stretch. We can define $q(s_0, t) = \partial s / \partial s_0$ as a local strain. It describes the local extension. The rate of CCR $k(s_0, t)$ can be written as the following form

$$k(s_0, t) = \boldsymbol{\kappa} : \mathbf{S}(s_0, t) q(s_0, t) - \frac{1}{q(s_0, t)} \frac{\partial q(s_0, t)}{\partial t}, \quad (1)$$

where $\boldsymbol{\kappa}$ is the velocity gradient tensor of the flow, which, we suppose, is homogeneous, although in general it is not; $\mathbf{S}(s_0, t)$ is the orientational tensor, $\mathbf{S}(s_0, t) \equiv \langle \mathbf{u}(s_0, t) \mathbf{u}(s_0, t) \rangle$. Apparently, it is a local approximation form. The first term in Eq. (1) describes the rate of entanglements convection at contour variable s_0 and t . The second term is used to exclude the case of affine deformation, in which there are no environment changes with respect to the primitive chain and no CCR happens. As $\mathbf{S}(\pm L_0/2, t) = 0$, $q(\pm L_0/2, t) = 1$, from Eq. (1)

we then find no CCR happens at the chain ends of the primitive chain. In fact the ends of the tube change instantaneously with the ends of the primitive chain during movement, there is no relative motion between the ends of the tube and the ends of the primitive chain. The primitive chain and the tube are intrinsically synonymous, we treat them as different things only for convenience in describing the motion of the chain considered and the motion of its surrounding chains.

The difficulty of the flow-reversal problem has been pointed out (Wapperom and Keunings, 2000; Ianniruberto and Marrucci, 2001). If the present model reduces to the uniform and single-relaxation-time version, this problem can be amended using the absolute value of $|\boldsymbol{\kappa} : \mathbf{S}|q$ in Eq. (1). In the present non-uniform case, we suppose that the above expression can amend this difficulty. In the following we will not write the absolute value sign in the rate of CCR by considering the flow only in one direction.

B. Segmental Stretch

The dynamics of segmental stretch is described by the equation of motion, in which we neglect the acceleration term. It is derived from the force balance between the segmental extension force caused by the flow and the entropic elastic force. If the chain is considered to be non-Gaussian, this equation can be written as (Mead and Leal, 1995a, b)

$$\frac{\partial}{\partial t}s(s_0, t) = \langle v(s_0, t) \rangle + \frac{3\beta Z D}{\alpha} \left[\frac{d}{dq} \mathcal{L}^{-1}(\alpha q) \right] \left(\frac{\partial^2 s}{\partial s_0^2} \right). \quad (2)$$

Here $\langle v(s_0, t) \rangle$ is the relative pre-averaged tangential velocity with respect to the center of chain

$$\langle v(s_0, t) \rangle = \boldsymbol{\kappa} : \int_0^{s_0} \mathbf{S}(s'_0, t) q(s'_0, t) ds'_0. \quad (3)$$

The parameter $Z = M/M_e$ is the number of entanglements in a primitive chain, where M_e is the molecular weight between two entanglements. $Z = T_d/3T_R$ (Doi and Edwards, 1986), where T_d is the reptation time and T_R is the Rouse relaxation time. D defines the diffusion coefficient along the primitive path, and is related to the reptation time by $T_d = L_0^2/\pi^2 D$.

β is a coefficient related to non-Gaussian behavior, which is given by

$$\beta = \frac{1 - \alpha^2}{3 - \alpha^2}, \quad (4)$$

where $\alpha = L_0/L_{max}$, and L_{max} is the maximum length the primitive chain can be stretched to. β ensures that the magnitude of a fictitious force acting along the primitive chain is equal to $3k_B T/a$ when there is no segmental extension (Doi and Edwards, 1986; Marrucci and Grizzuti, 1988). Here, a is the step length of the primitive chain and is a constant in the present model. A good discussion for its magnitude is given by Milner (2005). The inverse Langevin function $\mathcal{L}^{-1}(x)$ with the fractional extension $x = \alpha q$ is used to describe the tension of a non-Gaussian finitely extensible polymer segment (Treloar, 1975), which satisfies the following equation

$$\mathcal{L}(x) = \coth(x) - \frac{1}{x}. \quad (5)$$

Expanding $\mathcal{L}^{-1}(x)$ in a Taylor series and using Padé approximation (Cohen, 1991), we can obtain

$$\begin{aligned} \mathcal{L}^{-1}(x) &= 3x + \frac{9}{5}x^3 + \frac{297}{175}x^5 + \dots \\ &\simeq x \frac{3 - x^2}{1 - x^2}. \end{aligned} \quad (6)$$

We differentiate both sides of Eq. (2) with respect to s_0 and obtain

$$\frac{\partial q(s_0, t)}{\partial t} = \boldsymbol{\kappa} : \mathbf{S}(s_0, t)q + \frac{3ZD\beta}{\alpha} \frac{d\mathcal{L}^{-1}(\alpha q)}{dq} \frac{\partial^2 q}{\partial s_0^2} + \frac{3ZD\beta}{\alpha} \left[\frac{d^2}{dq^2} \mathcal{L}^{-1}(\alpha q) \right] \left(\frac{\partial q}{\partial s_0} \right)^2. \quad (7)$$

Insert Eq. (6) into the above equation, we obtain

$$\frac{\partial q}{\partial t} = \boldsymbol{\kappa} : \mathbf{S}q + 3ZD\beta \frac{3 + \alpha^4 q^4}{(1 - \alpha^2 q^2)^2} \frac{\partial^2 q}{\partial s_0^2} + 3ZD\beta \alpha \frac{4\alpha^3 q^3 + 12\alpha q}{(1 - \alpha^2 q^2)^3} \left(\frac{\partial q}{\partial s_0} \right)^2. \quad (8)$$

Taking into account the effect of CCR and following the argument by Mead, Larson and Doi (1998), finally we obtain

$$\begin{aligned} \frac{\partial q}{\partial t} &= 3ZD\beta \frac{3 + \alpha^4 q^4}{(1 - \alpha^2 q^2)^2} \frac{\partial^2 q}{\partial s_0^2} + 3ZD\beta \alpha \frac{4\alpha^3 q^3 + 12\alpha q}{(1 - \alpha^2 q^2)^3} \left(\frac{\partial q}{\partial s_0} \right)^2 \\ &\quad + \boldsymbol{\kappa} : \mathbf{S}q - \frac{1}{2} \left(\boldsymbol{\kappa} : \mathbf{S}q - \frac{1}{q} \frac{\partial q}{\partial t} \right) (q - 1). \end{aligned} \quad (9)$$

The parameter $1/2$ comes from the fact that the magnitude of the rate of entanglements reduction due to CCR is two times as large as the rate of segmental retraction. The boundary condition and the initial condition are

$$q(s_0, t)|_{s_0=\pm L_0/2} = 1$$

and

$$q(s_0, t)|_{t=0} = 1,$$

respectively. The boundary condition is specified by the untethered condition of the chain ends which can never be stretched.

C. Probability of Tube Survival

The process of the segmental orientation can be described by the tube survival probability $G(s, t, t')$, which means that a tube segment created at past time t' still can be found at location s and time t . In the original DE model, $G(s, t, t')$ satisfies a diffusion equation. When the segmental stretch is taken into account, such as the DEMG model, a convective term has to be added to the DE model. This term accounts for the flow induced convection of the *defects* to the ends of the primitive chain and the elongation of the tube segments. However, the orientation relaxation induced by constraint release has not been considered. Without that it makes the prediction of the rheological properties by these models qualitatively different from the experimental results.

Based on our understanding for the effect of constraint release, we modify the CCR term in the equation of the probability of tube survival in MLD model and drop the term which comes from the reptative constraint release. Including the contribution from chain stretch, the equation for the probability of the tube survival is given by

$$\frac{\partial G(s, t, t')}{\partial t} = D \frac{\partial^2 G(s, t, t')}{\partial s^2} - \langle v(s, t) \rangle \frac{\partial G(s, t, t')}{\partial s}, \quad (10)$$

where $s = s(s_0, t)$ is the tube strain function. The boundary condition and the initial

condition are

$$G(s, t, t')|_{s=\pm L/2} = 0$$

and

$$G(s, t, t')|_{t=t'} = 1,$$

respectively. It is convenient to transform the independent variables s and t to other independent variables s_0 and t (Pearson et al., 1991).

$$\frac{\partial G(s_0, t, t')}{\partial t} = \frac{D}{q^2} \frac{\partial^2 G(s_0, t, t')}{\partial s_0^2} + \left(-\frac{D}{q^3} \frac{\partial q}{\partial s_0} - \frac{1}{q} \langle v(s_0, t) \rangle + \frac{1}{q} \frac{\partial s}{\partial t} \right) \frac{\partial G(s_0, t, t')}{\partial s_0}, \quad (11)$$

where $q = q(s_0, t)$ is the function of local strain. When we consider the CCR mechanism, a new term must be added to Eq. (11), which is

$$\left(\boldsymbol{\kappa} : \mathbf{S}q - \frac{1}{q} \frac{\partial q}{\partial t} \right) G(s_0, t, t').$$

Here, \mathbf{S} is the orientational tensor. Then we obtain

$$\begin{aligned} \frac{\partial G(s_0, t, t')}{\partial t} = & \frac{D}{q^2} \frac{\partial^2 G(s_0, t, t')}{\partial s_0^2} + \left(-\frac{D}{q^3} \frac{\partial q}{\partial s_0} - \frac{1}{q} \langle v(s_0, t) \rangle + \frac{1}{q} \frac{\partial s}{\partial t} \right) \frac{\partial G(s_0, t, t')}{\partial s_0} \\ & - f \left(\frac{\partial s}{\partial s_0} \right) \left(\boldsymbol{\kappa} : \mathbf{S}q - \frac{1}{q} \frac{\partial q}{\partial t} \right) G(s_0, t, t'), \end{aligned} \quad (12)$$

where $f(\partial s / \partial s_0) = 1/q$ is the switch function (Mead et al., 1998). When q is large, the contribution from the last term in the right hand side of Eq. (12) is much smaller. However, when q approaches to unity, this term plays an important role. This is arisen from the large difference in the time scale between the reptation time and the Rouse retraction time. It means that the relaxation of the tube orientation caused by constraint release of surrounding chains should start to happen just when the primitive chain nearly finish its retraction. The boundary condition is

$$G(s_0, t, t')|_{s_0=\pm L_0/2} = 0,$$

and the initial condition is

$$G(s_0, t, t')|_{t=t'} = 1,$$

Note that $G(s_0, t, t')$ is the probability function, which has a range from 0 to 1.

D. Constitutive Equations

The stress is the sum of tensile force of the primitive chain projecting to some direction \mathbf{u} by averaging over the conformations of primitive chains. Those primitive chains penetrate a unit area plane with its normal direction \mathbf{u} . The tensile force acting on segment s_0 , along the non-Gaussian primitive chain at time t can be expressed by the inverse Langevin function

$$F(s_0, t) = \frac{k_B T}{a} \mathcal{L}^{-1} \left(\alpha \frac{\partial s}{\partial s_0} \right). \quad (13)$$

When the Padé approximation is used, we have

$$F(s_0, t) = \frac{3k_B T}{a} \beta \frac{3 - \alpha^2 q^2}{1 - \alpha^2 q^2}, \quad (14)$$

where β has the same meaning as in Eq. (4), and is used to conform that when $q = 1$, $F(s_0, t) = 3k_B T/a$ is equal to the fictitious force acting on every segment (Marrucci and Grizzuti, 1988). The stress can be written as

$$\begin{aligned} \boldsymbol{\sigma} &= \frac{c}{N} \left\langle \int_{-L/2}^{L/2} ds F(s_0, t) \mathbf{u}(s, t) \mathbf{u}(s, t) \right\rangle \\ &\simeq \frac{c}{N} \int_{-L/2}^{L/2} ds \langle F(s_0, t) \rangle \langle \mathbf{u}(s, t) \mathbf{u}(s, t) \rangle \\ &= \frac{15}{4} \frac{G_N^0}{L_0} \int_{-L_0/2}^{L_0/2} \beta \frac{3 - \alpha^2 q^2}{1 - \alpha^2 q^2} q^2 \mathbf{S}(s_0, t) ds_0, \end{aligned} \quad (15)$$

where c is the number of polymers in a unit volume and N being the degree of polymerization. We decouple the average segmental tension from the average segmental orientation in the calculation of the first line to the second line. G_N^0 is the plateau modulus, $G_N^0 = 4ck_B T L_0 / 5Na$. $\mathbf{S}(s_0, t)$ can be expressed by

$$\mathbf{S}(s_0, t) = \int_{-\infty}^t dt' \frac{\partial G(s_0, t, t')}{\partial t'} \mathbf{Q}(\mathbf{E}(t, t')). \quad (16)$$

Here, \mathbf{Q} is the DE strain tensor without the independent alignment approximation given by

$$\mathbf{Q} = \left\langle \frac{(\mathbf{E} \cdot \mathbf{u})(\mathbf{E} \cdot \mathbf{u})}{|\mathbf{E} \cdot \mathbf{u}|} \right\rangle_0 \frac{1}{\langle |\mathbf{E} \cdot \mathbf{u}| \rangle_0}, \quad (17)$$

where \mathbf{E} is the deformation tensor (Doi and Edwards, 1986).

III. RESULTS AND DISCUSSION

The results reported in this paper will focus on steady and start-up of simple shear flow of monodisperse concentrated polymeric systems. We scale the equations for simplicity. The time variable is scaled by the reptation time, $t/T_d \rightarrow t$, and the spatial variable is scaled by the length of primitive chain at equilibrium, $s_0/L_0 \rightarrow s_0$. For convenience, we use the same symbol to denote the scaled quantities. Eqs. (9), (12) and (15) become

$$\begin{aligned} \frac{\partial q}{\partial t} = & \frac{3Z\beta}{\pi^2} \frac{3 + \alpha^4 q^4}{(1 - \alpha^2 q^2)^2} \frac{\partial^2 q}{\partial s_0^2} + \frac{3Z\beta\alpha}{\pi^2} \frac{4\alpha^3 q^3 + 12\alpha q}{(1 - \alpha^2 q^2)^3} \left(\frac{\partial q}{\partial s_0} \right)^2 \\ & + \kappa : \mathbf{S}q - \frac{1}{2} \left(\kappa : \mathbf{S}q - \frac{1}{q} \frac{\partial q}{\partial t} \right) (q - 1), \end{aligned} \quad (18)$$

$$\begin{aligned} \frac{\partial G(s_0, t, t')}{\partial t} = & \frac{1}{\pi^2 q^2} \frac{\partial^2 G(s_0, t, t')}{\partial s_0^2} + \left(-\frac{1}{\pi^2 q^3} \frac{\partial q}{\partial s_0} - \frac{1}{q} \langle v(s_0, t) \rangle + \frac{1}{q} \frac{\partial s}{\partial t} \right) \frac{\partial G(s_0, t, t')}{\partial s_0} \\ & - \frac{1}{q} \left(\kappa : \mathbf{S}q - \frac{1}{q} \frac{\partial q}{\partial t} \right) G(s_0, t, t'), \end{aligned} \quad (19)$$

$$\boldsymbol{\sigma} = \int_{-1/2}^{1/2} \beta \frac{3 - \alpha^2 q^2}{1 - \alpha^2 q^2} q^2 \mathbf{S}(s_0, t) ds_0, \quad (20)$$

respectively. Here, $\langle v(s_0, t) \rangle$ is given by Eq. (3), the relationship of which before scaling and after scaling is $\langle v(s_0, t) \rangle T_d/L_0 \rightarrow \langle v(s_0, t) \rangle$. The stress tensor has been scaled as $4\boldsymbol{\sigma}/15G_N^0 \rightarrow \boldsymbol{\sigma}$. $\mathbf{S}(s_0, t)$ is given by Eq. (16). For the case of shear flow, $\kappa = \dot{\gamma} \hat{e}_y \hat{e}_x$. The shear viscosity is defined by $\eta = \sigma_{xy}/\dot{\gamma}$, where σ_{xy} is the shear stress and the primary normal stress coefficient is given by $\Psi = (\sigma_{xx} - \sigma_{yy})/\dot{\gamma}^2$, where $\sigma_{xx} - \sigma_{yy}$ is the first normal stress difference. The boundary conditions are

$$q(s_0, t)|_{s_0=\pm 1/2} = 1,$$

$$G(s_0, t, t')|_{s_0=\pm 1/2} = 0,$$

and the initial conditions are

$$q(s_0, t)|_{t=0} = 1,$$

$$G(s_0, t, t')|_{t=t'} = 1,$$

These equations are nonlinear and have to be solved numerically. Combining the finite differencing and the Newton-Raphson method, we can obtain the solutions of these equations.

The details are shown in the Appendix. The constitutive parameters in these equations include Z and α . Here, Z is the number of entanglements per chain and can be specified by fitting the steady state predictions of the model and the experimental data. A larger Z corresponds to a shorter Rouse relaxation time. α is the ratio between the equilibrium and the maximum length of the primitive chain, reflecting the extensibility of the chain.

A. Steady state shear flow

In this section, we show the dynamic properties of the chain segments and rheological behavior under steady shear flow.

Fig. 1 gives the non-uniform segmental stretch of the primitive chain with different shear rates. The parameters are chosen as $Z = 20$ and $\alpha = 0$ which denote the Gaussian chain. Due to the untethered fact of the chain ends, the segments at chain ends remain unstretched. There exists a maximum value of stretch at the center. The extension of the segments equivalently reduces the diffusion coefficient by $1/q^2$ in Eq. (19). So the equivalent reduction of diffusion is much more at the center. In addition to a small value of the rate of segmental convection around the center, we find that the rate of tube relaxation, or the rate of tube creation, is relatively small at the center. The cancellation of gradually increasing rate of convection and decreasing rate of effective diffusion from the center to ends induces a flat region of the rate of the tube relaxation around the center. According to the calculation from Eq. (16) under steady state shear, we find that around the center of the tube the value of S_{xy} is relatively small. At the ends, where the segments of tube disappear at their creating time, $S_{xy}(\pm 1/2, t) = 0$. Therefore, there must be a maximum value of S_{xy} in some location between the center and the ends. This can be seen from Fig. 2 when the shear rate is high enough. It is very interesting that when the shear rate is high enough, the maximum contribution to stress from segmental orientation comes neither from the ends of the chain nor from the center, but from some other location in between. Moreover, this location will move towards the ends when the shear rate grows higher. From the calculation we also

find that the segmental orientation is insensitive to the entanglement number of a primitive chain, denoted as Z which determines the segmental extension in steady state. Fig. 3 shows the differences of S_{xy} between the present model and DEMG model for $Z = 20$ and $Z = 50$, respectively. The result shows that including of the CCR term will obviously enhance the value of S_{xy} . Therefore, the magnitude of the stress in fast flow is seriously underestimated in the DEMG model.

The comparisons of the shear stress and the steady state shear viscosity with different values of Z are given in Fig. 4. In the linear region, where the steady shear rate is smaller than the inverse of reptation time, both the shear stresses and steady state shear viscosity are independent of Z , because in these cases the shear rates are not high enough to stretch the chain segments. When the shear rate is high enough, the segments will be stretched to many times of their equilibrium length. The larger extension of the segment is, the more it contributes to the shear stress. On the other hand, the Rouse relaxation time T_R determines the magnitude of segmental extension. If T_R is larger, which corresponds to a smaller Z , the shear stress will be larger. Fig. 4 also shows the shear viscosity of the steady state which is defined as $\eta(\dot{\gamma}) = \sigma_{xy}/\dot{\gamma}$. When the shear rate is smaller than the inverse of reptation time, it behaves as Newtonian fluid. While in the high-shear-rate region it markedly depends on the shear rate. Different segmental stretch results in the differences of the first normal stress difference in the high-shear-rate region, which can be seen in Fig. 5. The same characteristics for the primary normal stress coefficients are also shown in Fig. 5.

Up to now the chains are approximated as Gaussian chains ($\alpha = 0$), which is valid if the stains are not too large. However, under fast flow the chains are largely stretched and approach to their limiting extensible values, the Gaussian treatment is no longer valid. In the following, we will use the non-Gaussian treatment of the single chain taking into account the finite extensibility of the chain ($\alpha \neq 0$). Fig. 6 shows the comparisons of the shear stress and the first normal stress difference with respect to the shear rate with different extensibilities for $\alpha = 0, 0.2, 0.4$ and 0.6 , respectively. The parameter Z is chosen as $Z = 20$. The calculation also indicates that for a specified value of the shear rate segmental orientation is

not sensitive to segmental extensibility. From Fig. 6 it can be found that the curves of shear stress and first normal stress difference are independent of segmental extensibility in the small shear rate region where the stress contribution from segmental stretch can be ignored. In the high-shear-rate region, the differences of shear stress and the differences of the first normal stress caused by the differences of segmental extensibility are mainly contributed from segmental extension. The segmental orientation is only determined by the value of the shear rate, and is independent of the segmental stretch, because they are considered as independent processes.

Fig. 6 also shows the comparisons between the predictions of the present model and the experimental data (Pattamaprom and Larson, 2001) of the stresses and the first normal stress differences under steady shear for different parameters of α ; Fig. 7 shows the comparisons with experimental data of the stresses and the first normal stress differences under steady shear for different parameters of Z . By fitting the experimental data, we find that incorporating the non-uniform features to the constitutive models does not affect rheological properties. Moreover, the non-uniform model gives us the detailed descriptions of the chain dynamics. In the present model there are two modifiable parameters of Z and α . By fitting the experimental data to the predictions of the present model, we can obtain the values of Z and α , respectively. The comparison between them will show you the relative abilities of the retraction and the extension of the chains. This means that, under the same magnitude of shear rate, different abilities of retraction or extension will result in different magnitudes of stresses, although the molecules composing the materials may have the same volume fractions and molecular weights. From these two figures, quantitative deviation from the experimental data exists, especially the first normal stress difference in the high-shear-rate region. These deviations may attribute to the “nonlocal” interactions between chains. By comparing with the uniform models by Pattamaprom and Larson (2001), we also find that the effect of non-uniform CCR on the stress and the normal stress is minor. The details of segmental orientation and stretch are not important in determining the rheological properties in steady simple shear.

B. Start-up of Steady Shear Flow

The transient behavior of chain stretch and orientation, as well as the rheological properties, are discussed in this section. The steady shear is imposed to the system at $t = 0$.

In Fig. 8 the segmental stretch varying with time at different shear rates are shown, and the constitutive parameters are chosen as $Z = 20, \alpha = 0.0$. The contour variable is focused at $s_0 = 0$. Before this segment reaches its steady value of extension, it passes a maximum value which is dependent on the shear rate, since other parameters are fixed. This maximum value will appear earlier when the shear rate increases. Fig. 9 gives the behavior of segmental orientation $S_{xy}(0, t)$ with the constitutive parameters chosen as the same in Fig. 8. We focus on the location $s_0 = 0$. If the shear rate is of the order of $1/T_d$ or larger, the value of $S_{xy}(0, t)$ will also pass a maximum value before reaching its steady value. The appearance of the maximum value is not due to the fact of segmental stretch, but the existence of a maximum value in the strain Q_{xy} with respect to the time.

Fig. 10 and Fig. 11 show the transient behavior of the shear stress and the first normal stress difference, respectively, where overshoots are predicted in the present model. For the shear stress, when the shear rate is higher than the inverse of reptation time, the overshoot appears. The overshoot of the first normal stress difference appears at a much higher shear rate in the present model than that in other models. The reason is that the appearance of maximum in the first normal stress difference is determined by the evolvement of segmental stretch which should also have a maximum in the course of time. However, the rate of CCR we obtained contains a local strain $q(s, t)$, which largely decreases the maximum value of segmental stretch and subsequently the stress. Thus the magnitude of the start-up shear rate, which can produce a overshoot, increases.

Fig. 12 and Fig. 13 show the comparisons of the shear viscosities and the first normal stress differences with the experimental results, respectively. We choose the shear viscosities instead of the shear stresses for convenience to compare with the experimental data (Pattamaprom and Larson, 2001), in which the material is sample one. The parameters in

these two figures are both chosen as $Z = 20$ and $\alpha = 0, 0.3, 0.6$, respectively. The results indicate that only when the shear rate is high, i.e. $\dot{\gamma} \geq 10/T_d$, the differences caused by the different values of α are predicted by the present model. If the chains are less extensible, which corresponds to a large value of α , the segmental extension will be smaller under the same shear rate at the same time. This leads to smaller shear viscosities as well as the first normal stress differences. In fact, the segmental orientation is mainly determined by the magnitude of the start-up shear rate. When the shear rate is fixed the contribution from orientation to shear stress is specified. Thus, the magnitude of segmental stretch plays a critical role in determining the final value of the shear stress, and subsequently the shear viscosity. This is kept when the first normal stress difference is considered. By fitting the experimental data we find that the predictions of the present model have the same tendency with the experimental curves. On the other hand, there are large inconsistencies when the quantitative values are concerned, especially the magnitude of overshoots. Both the shear stress and the normal stress overshoots in the present model are very weak comparing to the experimental data. It is obvious that the chain stretch is not enough, which may arise from the inclusion of local approximation in CCR in the present model.

IV. CONCLUSIONS

In this paper, we develop a contour-variable model to describe the non-uniform behavior of segments under steady shear and start-up of steady shear, and the subsequent contributions to the shear stress and the first normal stress difference. The present model is a modification of the MLD model with a modified CCR term and non-Gaussian chain treatment of the single chain. We drop the contour length fluctuation contribution and neglect the reptative constraint release term, since both of them contribute less than the shear rate dependent CCR term in the high-shear-rate region. The numerical results predict strong dependencies of the segmental stretch and orientation on the contour variable. The maximum extension happens in the center of the chain due to the demand of symmetry. The fact that segmental

extension passes a maximum during the start-up of steady shear flow is the key reason why the first normal stress difference has a maximum. The segmental orientation also shows a maximum in the center when shear rate is small, and this is mainly attributed to the reptation. However, when the shear rate is high enough the segmental convection begins to work. A maximum of segmental orientation appears in some locations between the center and the end, where the stress contribution from orientation is the largest. The inclusion of CCR entirely promotes the magnitude of orientation of each segment rather than changes the distribution of the value of segmental orientation. The non-uniform segmental orientation and stretch subsequently contribute to rheological properties, which qualitatively agree with experimental data, although quantitative deviation still exists. When the shear rate is high, i.e. $\dot{\gamma} \gg T_d^{-1}$, the segmental strain is larger than 1. The difference of the segmental extensibilities is the main reason for the difference of rheological behavior. The same properties hold in the start-up of steady shear. This validates our pre-approximation of the independence of segmental stretch and orientation.

A few approximations have been used in the present model. One is the local approximation of CCR. CCR happens once a tube segment is convected away from its original location, since the relative position to the primitive-chain segment confined by this tube segment changes. The convection of a segment may not be only determined by its local conditions, but all other segments elsewhere. In fact, the present model only predicts the overshoots in shear viscosity and first normal stress difference under the start-up of steady shear, but does not predict undershoots which have been observed in experiments (Huppler et al., 1967; Mhetar and Archer, 2000). It is well known that the appearance of overshoots is due to segmental stretch. How about the undershoots? Pattamaprom and Larson (2001) predicted that the undershoots would appear if the dependence of the orientation and stretch on the contour variable was taken into account. The present model indicates that the inclusion of “local” non-uniform rate of CCR to the constitutive equations does not predict undershoots. Undershoots may appear if we include the nonlocal interaction into the model. That is the coupling between chains, e.g. the hydrodynamic interactions,

which are neglected in the present model. Another is that we suppose the shear flow is homogeneous, which in general is not. At last we can say that in polymer melts under shear non-uniform segmental orientation and stretch are hard to be observed directly in experiments, but their effect on rheological behavior can be detected, though the influences of the microscopic non-uniform behavior on them is not remarkable. However, the processes of crystallization and the dynamics of phase separation (Maurits and Fraaije, 1997) should be significantly affected by these contour dependent quantities, as the segmental dynamics plays a crucial rule in these processes. In fact the kinetic coefficients are related to the non-uniform features (Kawasaki and Sekimoto, 1988; Kawakatsu, 1997). It is of great significance to investigate the segmental dynamics and their affiliated properties theoretically by microscopic or mesoscopic models.

ACKNOWLEDGMENTS

We thank Dr. Bing Miao for the helpful discussion and suggestions. This work is supported by National Natural Science Foundation of China (NSFC) 20490222, 20874111, 50821062 and the Grant from Chinese Academy of Sciences KJCX2-YW-206.

APPENDIX A

In this Appendix we describe the process and methods for the calculation of constitutive equations. The DE strain tensor without the independent alignment approximation, i.e. Eq. (17), is integrated numerically. The unit vector of orientation is chosen as $\mathbf{u} = (\sin \theta \cos \varphi, \sin \theta \sin \varphi, \cos \theta)$

$$\begin{aligned} Q_{xy} &= \left\langle \frac{(\mathbf{E} \cdot \mathbf{u})_x (\mathbf{E} \cdot \mathbf{u})_y}{|\mathbf{E} \cdot \mathbf{u}|} \right\rangle_0 \frac{1}{\langle |\mathbf{E} \cdot \mathbf{u}| \rangle_0} \\ &= \left\langle \frac{(u_x + \gamma u_y) \cdot u_y}{(1 + 2\gamma u_x u_y + \gamma^2 u_y^2)^{1/2}} \right\rangle_0 \frac{1}{\langle (1 + 2\gamma u_x u_y + \gamma^2 u_y^2)^{1/2} \rangle_0}, \end{aligned} \quad (\text{A1})$$

where γ is the shear deformation, $\langle \dots \rangle_0$ denotes the average over the isotropic state, i.e., $\langle \dots \rangle_0 = \int d\mathbf{u} / 4\pi (\dots)$. Then we have

$$\begin{aligned} \alpha(\gamma) &\equiv \langle (1 + 2\gamma u_x u_y + \gamma^2 u_y^2)^{1/2} \rangle_0 \\ &= \frac{1}{4\pi} \int_0^\pi \sin \theta d\theta \int_0^{2\pi} d\varphi (1 + 2\gamma \sin^2 \theta \sin \varphi \cos \varphi + \gamma^2 \sin^2 \theta \sin^2 \varphi)^{1/2} \\ &= \int_0^1 dx \int_0^1 dy \left[1 + \frac{1}{2} \gamma^2 (1 - x^2) + \gamma (1 - x^2) \sin(4\pi y) - \frac{1}{2} \gamma^2 (1 - x^2) \cos(4\pi y) \right]^{1/2} \end{aligned} \quad (\text{A2})$$

Here, the variable transformations, i.e. $x = \cos \theta$, $y = \varphi / 2\pi$, are introduced. Then we have

$$Q_{xy} = \frac{1}{\alpha(\gamma)} \frac{1}{2} \int_0^1 dx \int_0^1 dy \frac{(1 - x^2) \sin(4\pi y) + \gamma (1 - x^2) - \gamma (1 - x^2) \cos(4\pi y)}{\left[1 + \frac{1}{2} \gamma^2 (1 - x^2) + \gamma (1 - x^2) \sin(4\pi y) - \frac{1}{2} \gamma^2 (1 - x^2) \cos(4\pi y) \right]^{1/2}}. \quad (\text{A3})$$

With the same procedure, we obtain

$$\begin{aligned} Q_{xx} - Q_{yy} &= \frac{1}{\alpha(\gamma)} \int_0^1 dx \int_0^1 dy \\ &\times \frac{\left(1 - \frac{1}{2} \gamma^2\right) (1 - x^2) \cos(4\pi y) + \gamma (1 - x^2) \sin(4\pi y) + \frac{1}{2} \gamma^2 (1 - x^2)}{\left[1 + \frac{1}{2} \gamma^2 (1 - x^2) + \gamma (1 - x^2) \sin(4\pi y) - \frac{1}{2} \gamma^2 (1 - x^2) \cos(4\pi y) \right]^{1/2}}. \end{aligned} \quad (\text{A4})$$

The two-dimensional integrals of Eqs. (A2)-(A4) are integrated out using the extended *Simpson's rule* in each dimension, respectively.

The constitutive equations under start-up of steady shear are solved numerically. We discretize Eq. (18) using the Crank-Nicolson scheme, and define F as

$$F = u(i, j + 1) - q(i, j + 1) + u(i, j) + q(i, j), \quad (\text{A5})$$

where i and j denote the discretized contour variable grid points and time variable grid points, respectively. Here, $u(i, j)$ is given by

$$\begin{aligned}
u(i, j) = & \frac{3Z\beta}{\pi^2} \frac{\Delta t}{(\Delta s)^2} \frac{3 + \alpha^4 q^4(i, j)}{[1 - \alpha^2 q^2(i, j)]^2} \frac{q(i, j)}{1 + q(i, j)} [q(i + 1, j) - 2q(i, j) + q(i - 1, j)] \\
& + \frac{3Z\beta\alpha}{\pi^2} \frac{\Delta t}{(\Delta s)^2} \frac{4\alpha^3 q^3(i, j) + 12\alpha q}{[1 - \alpha^2 q^2(i, j)]^3} \frac{q(i, j)}{1 + q(i, j)} \frac{[q(i + 1, j) - q(i - 1, j)]^2}{4} \\
& + \frac{1}{2} \Delta t \dot{\gamma} S_{xy}(i, j) \frac{3q^2(i, j) - q^3(i, j)}{1 + q(i, j)}
\end{aligned} \tag{A6}$$

where Δs and Δt are the contour and time grid steps, respectively. The contour grid step is a constant in our calculation, while there are two kinds of time step if the shear rate is higher than $10/T_d$. The grids density around the maximum value of $Q_{xy}(\gamma)$ is larger than that the place far from it, so that the effects arising from the sharp changes of the value of $Q_{xy}(\gamma)$ around the maximum value can be observed. There are $N_s - 1$ coupled equations if we set $F = 0$ for each time grid, and N_s is the grid number of of the contour coordinate. The Newton-Raphson method is used to find their roots at each time grid. The number of time step is N_t . In this paper, we choose $\Delta s = 5 \times 10^{-3}$ and Δt has a range from 5×10^{-6} to 4×10^{-4} depending on the shear rate. For a larger shear rate, we choose a smaller Δt . N_t is determined by the time grid steps. Eq. (19) can be written as

$$\frac{\partial G(s_0, t)}{\partial t} = A_0(s_0, t) \frac{\partial^2 G(s_0, t)}{\partial s_0^2} - A_1(s_0, t) \frac{\partial G(s_0, t)}{\partial s_0} + A_3(s_0, t) G(s_0, t), \tag{A7}$$

where

$$\begin{aligned}
A_0(s_0, t) &= 1/(\pi^2 q^2), \\
A_1(s_0, t) &= \left(\frac{1}{\pi^2 q^3} \frac{\partial q}{\partial s_0} + \frac{1}{q} \langle v(s_0, t) \rangle - \frac{1}{q} \frac{\partial s}{\partial t} \right), \\
A_3(s_0, t) &= -\frac{1}{q} \left(\boldsymbol{\kappa} : \mathbf{S} \mathbf{q} - \frac{1}{q} \frac{\partial q}{\partial t} \right).
\end{aligned}$$

Eq. (A7) can be discretized as

$$\begin{aligned}
\frac{G(i, j + 1) - G(i, j)}{\Delta t} = & A_0(i, j + 1) \frac{1}{2} \left[\left(\frac{\partial^2 G}{\partial s_0^2} \right)_{(i, j)} + \left(\frac{\partial^2 G}{\partial s_0^2} \right)_{(i, j+1)} \right] \\
& - A_1(i, j + 1) \frac{1}{2} \left[\left(\frac{\partial G}{\partial s_0} \right)_{(i, j)} + \left(\frac{\partial G}{\partial s_0} \right)_{(i, j+1)} \right] \\
& + A_3(i, j + 1) \frac{1}{2} (G(i, j) + G(i, j + 1)),
\end{aligned} \tag{A8}$$

where

$$\begin{aligned}\left(\frac{\partial^2 G}{\partial s_0^2}\right)_{(i,j)} &= \frac{G(i+1, j) - 2G(i, j) + G(i-1, j)}{(\Delta s)^2}, \\ \left(\frac{\partial G}{\partial s_0}\right)_{(i,j)} &= \frac{G(i+1, j) - G(i-1, j)}{2\Delta s}.\end{aligned}$$

The complete procedure is as follows. For every time step, we first assume that $S_{xy}(i, j+1) = S_{xy}(i, j)$. We solve the nonlinear equations of $F = 0$ (F is given by Eq. (A5)), then we obtain $q(i, j+1)$. Insert these into Eq. (A8) we obtain $G(i, j+1)$. From Eq. (16) we obtain the new values of $S_{xy}(i, j+1)$. By inserting these values back to Eq. (A5) and let $F = 0$, we obtain the new values of $q(i, j+1)$, then new $G(i, j+1)$, and subsequently $S_{xy}(i, j+1)$. Repeat the above steps until the expected convergent value (10^{-12}) is reached. The calculation of constitutive equations under steady shear is much easier than that under the start-up of steady shear, as in the former case the orientational tensor \mathbf{Q} and strain q are time independent, and the calculation procedure are the same as in the case of start-up of steady shear at a certain time grid.

References

- Cohen A (1991) A Padé approximant to the inverse Langevin function. *Rheol Acta* 30: 270-273
- de Gennes PG (1971) Reptation of a polymer chain in the presence of fixed obstacles. *J Chem Phys* 55: 572-579
- de Gennes PG (1979) *Scaling concepts in polymer physics*. Cornell University Press
- des Cloizeaux J (1988) Double reptation vs. simple reptation in polymer melts. *Europhys Lett* 5: 437-442
- des Cloizeaux J (1990) Relaxation of entangled polymers in melts. *Macromolecules* 23: 3992-4006
- Doi M (1980) A constitutive equation derived from the model of Doi and Edwards for concentrated polymer solutions and polymer melts. *J Polym Sci Polym Phys Ed* 18: 2055-2067
- Doi M, Edwards SF (1978a) Dynamics of concentrated polymer systems. Part 1.—Brownian motion in the equilibrium state. *J Chem Soc Faraday Trans II* 74: 1789-1801
- Doi M, Edwards SF (1978b) Dynamics of concentrated polymer systems. Part 2.—Molecular motion under flow. *J Chem Soc Faraday Trans II* 74: 1802-1817
- Doi M, Edwards SF (1978c) Dynamics of concentrated polymer systems. Part 3.—The constitutive equation. *J Chem Soc Faraday Trans II* 74: 1818-1832
- Doi M, Edwards SF (1979) Dynamics of concentrated polymer systems. Part 4.—Rheological properties. *J Chem Soc Faraday Trans II* 75: 38-54
- Doi M, Edwards SF (1986) *The theory of polymer dynamics*. Oxford Science Publications
- Graham RS, Likhtman AE, Mcleish TCB, Milner ST (2003) Microscopic theory of linear, entangled polymer chains under rapid deformation including chain stretch and convective constraint release. *J Rheol* 47: 1171-1200
- Huppler JD, Macdonald IF, Ashare E, Spriggs TW, Bird RB (1967) Rheological properties of three solutions. Part II. relaxation and growth of shear and normal stresses. *Trans Soc Rheol* 11: 181-204
- Ianniruberto G, Marrucci G (1996) On compatibility of the Cox-Merz rule with the model of Doi and Edwards. *J Non-Newtonian Fluid Mech* 65: 241-246
- Ianniruberto G, Marrucci G (2000) Convective orientational renewal in entangled polymers. *J Non-Newtonian Fluid Mech* 95: 363-374
- Ianniruberto G, Marrucci G (2001) A simple constitutive equation for entangled polymers with chain stretch. *J Rheol* 45: 1305-1318
- Janeschitz-Kriegl H (1982) *Polymer melt rheology and flow birefringence*. Springer-Verlag, Berlin
- Kawakatsu T (1997) Effects of changes in the chain conformation on the kinetics of order-disorder transitions in block copolymer melts. *Phys Rev E* 56: 3240-3250
- Kawasaki K, Sekimoto K (1988) Morphology dynamics of block copolymer systems. *Physica* 143A: 361-413
- Larson RG (1984) A constitutive equation for polymer melts based on partially

- extending strand convection. *J Rheol* 28: 545-571
- Larson RG (1988) Constitutive equations for polymer melts and solutions. Butterworths. Guildford
- Leygue A, Bailly C, Keunings R (2005) A differential formulation of thermal constraint release for entangled linear polymers. *J Non-Newtonian Fluid Mech* 128: 23-28
- Leygue A, Bailly C, Keunings R (2006a) A differential tube-based model for predicting the linear viscoelastic moduli of polydisperse entangled linear polymers. *J Non-Newtonian Fluid Mech* 133: 28-34
- Leygue A, Bailly C, Keunings R (2006b) A tube-based constitutive equation for polydisperse entangled linear polymers. *J Non-Newtonian Fluid Mech* 136: 1-16
- Marrucci G (1985) Relaxation by reptation and tube enlargement: a model for polydisperse polymers. *J Polym Sci Polym Phys Ed.* 23: 159-177
- Marrucci G (1986) The Doi-Edwards model without independent alignment. *J Non-Newtonian Fluid Mech* 21: 329-336
- Marrucci G (1996) Dynamics of entanglements a nonlinear model consistent with the Cox-Merz rule. *J Non-Newtonian Fluid Mech* 62: 279-289
- Marrucci G, Greco F, Ianniruberto G (2001) Integral and differential constitutive equations for entangled polymers with simple versions of CCR and force balance on entanglements. *Rheol Acta* 40: 98-103
- Marrucci G, Grizzuti N (1988) Fast flows of concentrated polymers predictions of the tube model on chain stretching. *Gazz Chim Ital* 118: 179-185
- Maurits NM, Fraaije JGEM (1997) Mesoscopic dynamics of copolymer melts: from density dynamics to external potential dynamics using nlocal kinetic coupling. *J Chem Phys* 107: 5879-5889
- Mead DW, Larson RG, Doi M (1998) A molecular theory for fast flows of entangled polymers. *Macromolecules* 31: 7895-7914
- Mead DW, Leal LG (1995a) The reptation model with segmental stretch I. basic equations and general properties. *Rheol Acta* 34: 339-359
- Mead DW, Leal LG (1995b) The reptation model with segmental stretch II. steady flow properties. *Rheol Acta* 34: 360-383
- Mhetar VR, Archer LA (2000) A new proposal for polymer dynamics in steady shearing flows. *J Polym Sci Part B Polym Phys* 38: 222-233
- Milner ST (2005) Predicting the tube diameter in melts and solutions. *Macromolecules* 38: 4929-4939
- Milner ST, Mcleish TCB, Likhtman AE (2001) Microscopic theory of convective constraint release. *J Rheol* 45: 539-563
- Pattamaprom C, Larson RG (2001) Constraint release effects in monodisperse and bidisperse polystyrenes in fast transient shearing flows. *Macromolecules* 34: 5229-5237
- Pearson DS, Helfand E (1984) Viscoelastic properties of star-shaped polymers. *Macromolecules* 17: 888-895
- Pearson DS, Herbolzheimer EA, Grizzuti N, Marrucci G (1991) Transient behavior of entangled polymers at high shear rates. *J Poly Sci Phys Ed* 29: 1589-1597

- Pearson DS, Kiss AD, Fetters LJ, Doi M (1989) Flow-induced birefringence of concentrated polyisoprene solutions. *J Rheol* 33: 517-535
- Treloar LRG (1975) *The physics of rubber elasticity*, 3rd edn. Clarendon Press. Oxford
- Viovy JL, Monnerie L, Tassin JF (1983) Tube relaxation: a necessary concept in the dynamics of strained polymers. *J Polym Sci Polym Phys Ed* 21: 2427-2444
- Wapperom P, Keunings R (2000) Simulation of linear polymer melts in transient complex flow. *J Non-Newtonian Fluid Mech* 95: 67-83
- Watanabe H (1999) Viscosity and dynamics of entangled polymers. *Prog Polym Sci* 24: 1253-1403

Figure Captions

Fig. 1 Non-uniform segmental stretch with different shear rates under steady shear. $\dot{\gamma}=0.1, 1, 10, 100, 500$, respectively, and $Z = 20, \alpha = 0$.

Fig. 2 Non-uniform segmental orientation with different shear rates under steady shear. $\dot{\gamma}=0.001, 0.1, 1, 10, 100, 500$, respectively, and $Z = 20, \alpha = 0$.

Fig. 3 Comparison of non-uniform segmental orientation of DEMG model and the present model under steady shear for $\alpha = 0$ and $Z=20, 50$, respectively.

Fig. 4 Steady shear viscosity and shear stress for $\alpha = 0$ and $Z=10, 20, 30, 50$, respectively.

Fig. 5 First normal stress differences and primary normal stress coefficients under steady shear for $\alpha = 0$ and $Z=10, 20, 30, 50$, respectively .

Fig. 6 Comparison of the stresses and the first normal stress differences under steady shear between the present model (lines) and the experimental data (closed symbols). The parameters are chosen as $Z = 20$ and $\alpha = 0, 0.2, 0.4, 0.6$, respectively.

Fig. 7 Comparison of the stresses and the first normal stress differences under steady shear between the present model (lines) and the experimental data (closed symbols). The parameters are chosen as $\alpha = 0$ and $Z = 10, 20, 30, 50$, respectively.

Fig. 8 The transient behavior of segmental stretch at $s_0 = 0$ for $\dot{\gamma}=0.1, 1, 10, 50, 100$, respectively, and $Z = 20, \alpha = 0$.

Fig. 9 The transient behavior of segmental orientation at $s_0 = 0$ for $\dot{\gamma}=0.01, 0.1, 1, 10, 100, 200$, respectively, and $Z = 20, \alpha = 0$.

Fig. 10 The transient behavior of shear stress under different shear rates for $\dot{\gamma}=0.001, 0.01, 0.1, 1, 10, 100$, respectively, and $Z = 20, \alpha = 0$.

Fig. 11 The transient behavior of the first normal stress differences under different shear rates for $\dot{\gamma}=0.1, 1, 10, 100, 200$, respectively, and $Z = 20, \alpha = 0$.

Fig. 12 Comparison of the shear viscosities with the experimental data (closed symbols). The parameters are chosen as $Z = 20$ and $\alpha = 0, 0.3, 0.6$, respectively.

Fig. 13 Comparison of the first normal stress differences with the experimental data (closed symbols). The parameters are chosen as the same as those in Fig. 12.

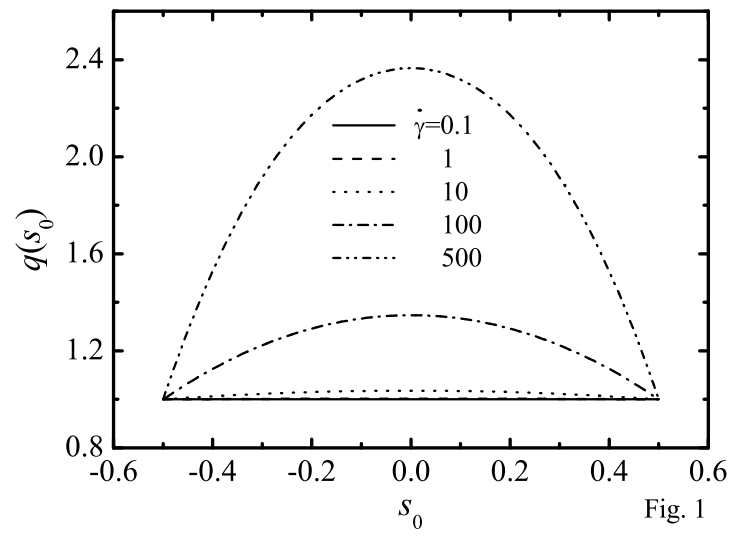
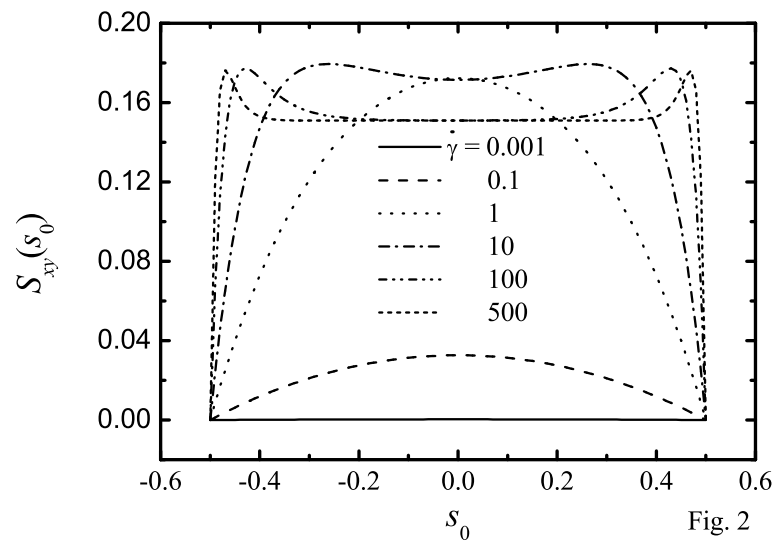


Fig. 1



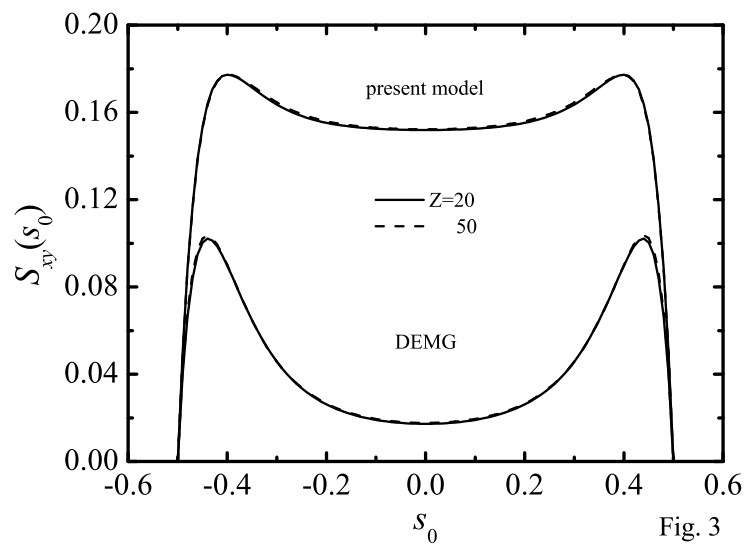


Fig. 3

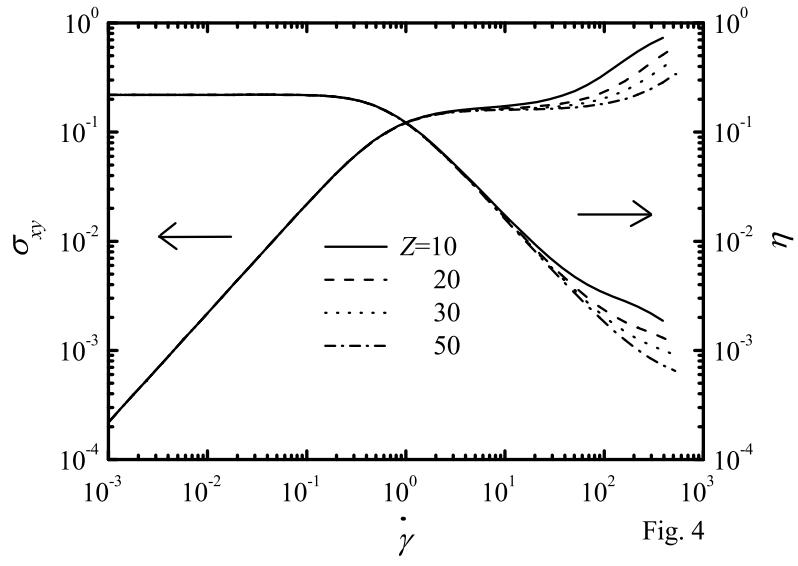
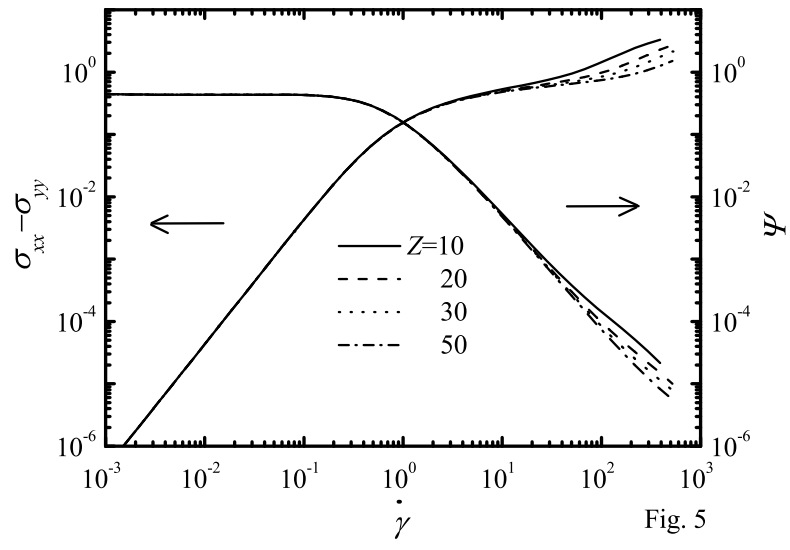
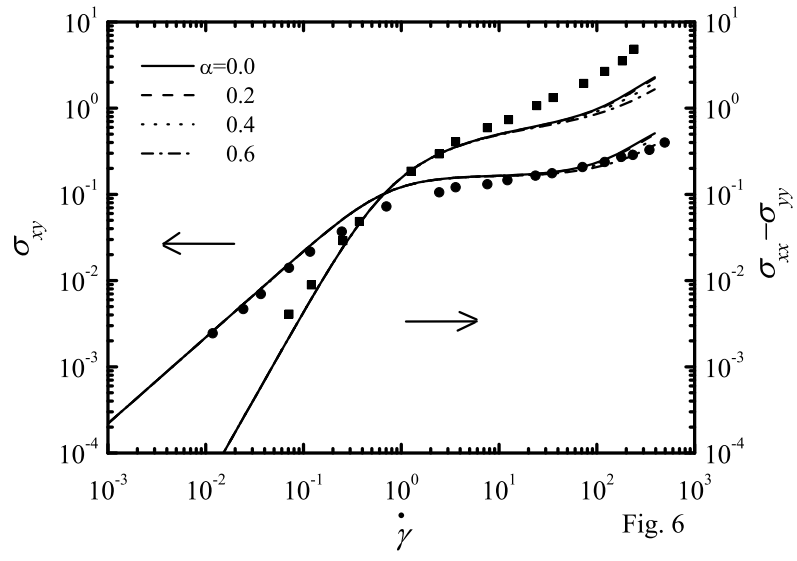


Fig. 4





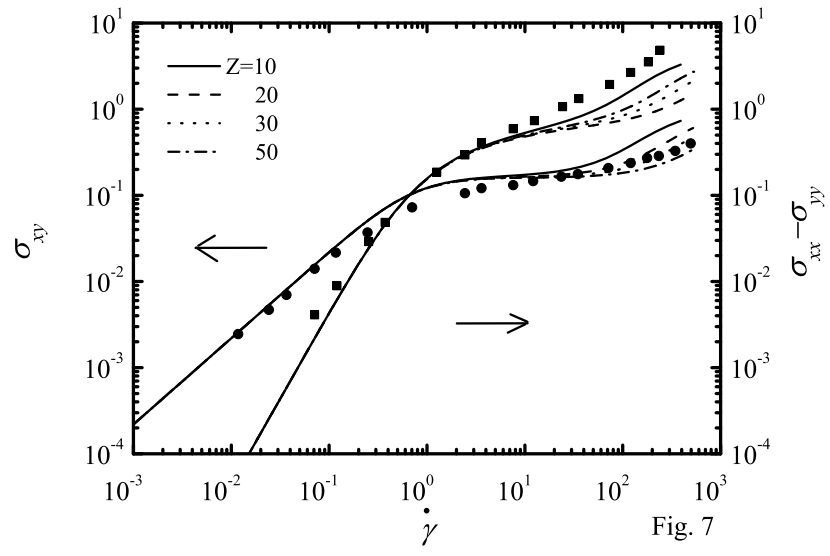


Fig. 7

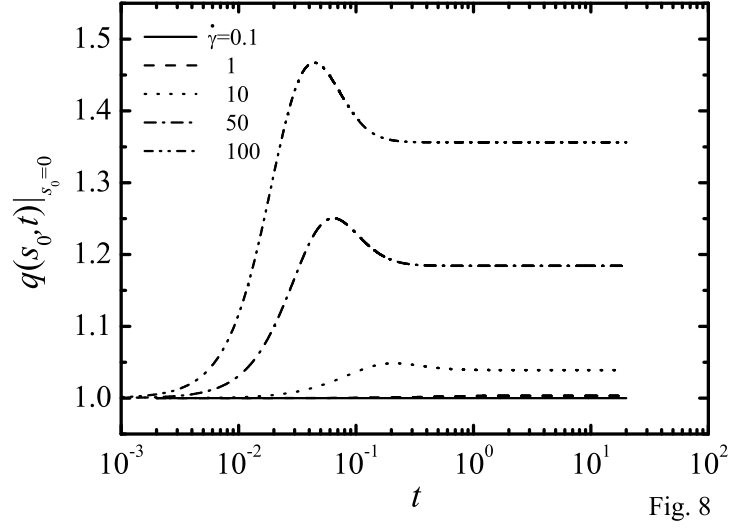


Fig. 8

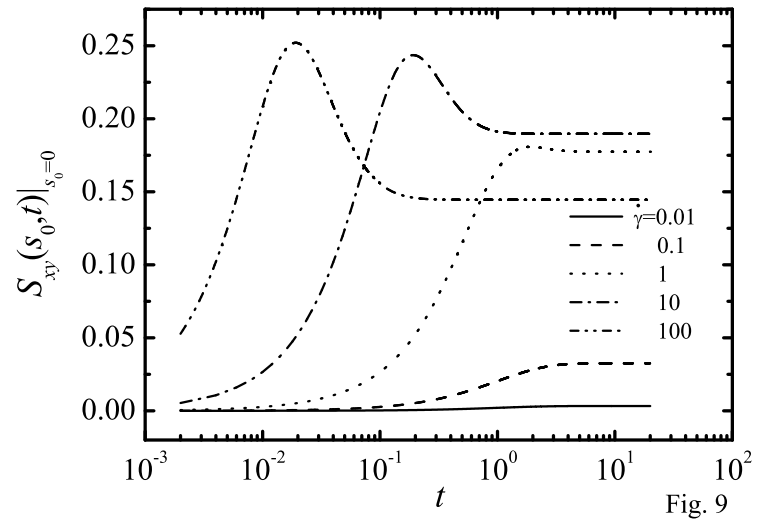
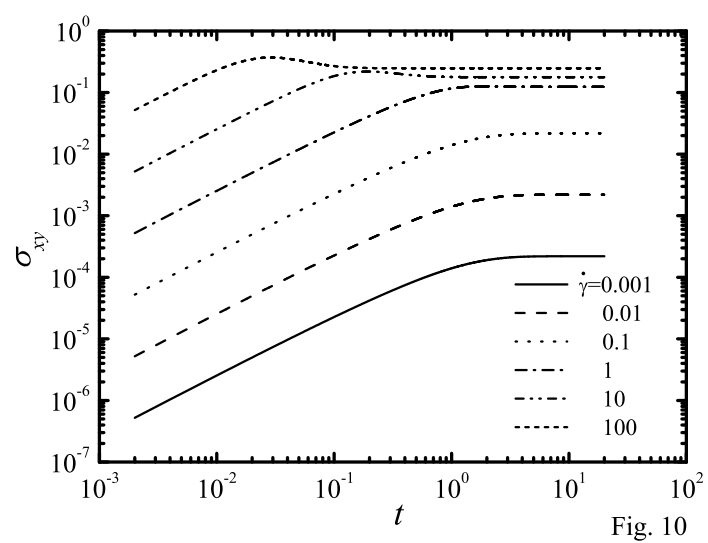
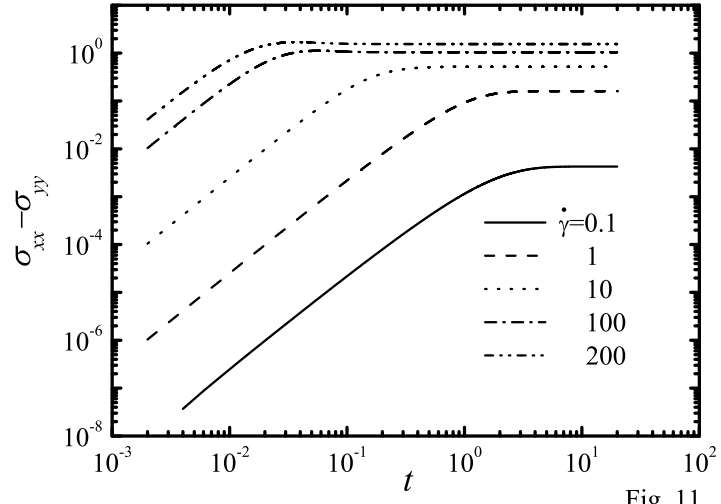
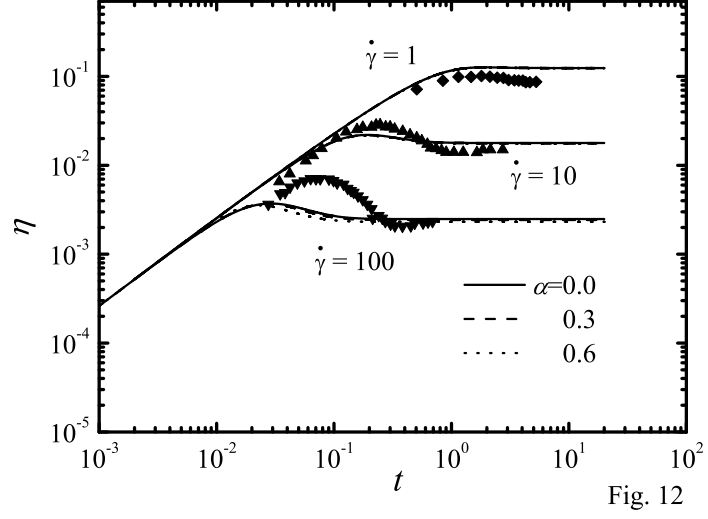


Fig. 9







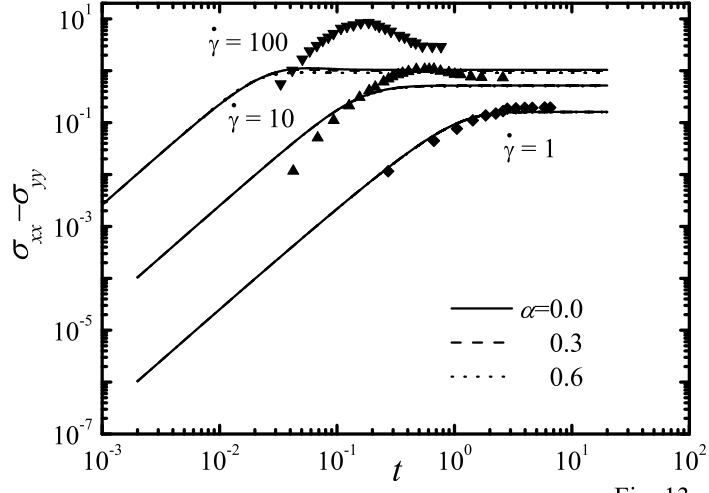


Fig. 13